J|A|C|S
ARTICLES
Published on Web 12/12/2007

Rationally Designed Ligands that Inhibit the Aggregation of Large Gold Nanoparticles in Solution

Shishan Zhang, Gyu Leem, La-ongnuan Srisombat, and T. Randall Lee*

Departments of Chemistry and Chemical Engineering, University of Houston, 4800 Calhoun Road, Houston, Texas 77204-5003

Received April 8, 2007; Revised Manuscript Received October 25, 2007; E-mail: trlee@uh.edu

Abstract: Hexadecanethiol (***n*-C16**), 2,2-dimethylhexadecane-1-thiol (**DMC16**), and the multidentate thiol-based ligands 2-tetradecylpropane-1,3-dithiol (**C16C2**), 2-methyl-2-tetradecylpropane-1,3-dithiol (**C16C3**), and 1,1,1-tris(mercaptomethyl)pentadecane (***t*-C16**) were evaluated for their ability to stabilize large gold nanoparticles (>15 nm) in organic solution. Citrate-stabilized gold nanoparticles (20−50 nm) treated with the ligands were extracted from aqueous solution and dispersed into toluene. The degree of aggregation of the gold nanoparticles was monitored visually and further confirmed by UV−vis spectroscopy and dynamic light scattering (DLS). The bidentate ligands (**C16C2** and **C16C3**) and particularly the tridentate ligand (***t*-C16**) showed enhanced abilities to inhibit the aggregation of large gold nanoparticles in organic solution. For gold nanoparticles modified with these multidentate ligands, bound thiolate ($S_{2p3/2}$ binding energy of 162 eV) was the predominant sulfur species (>85%) as evaluated by X-ray photoelectron spectroscopy (XPS). Although an entropy-based resistance to ordering of the loosely packed surfactant layers was initially considered to be a plausible mechanism for the enhanced stabilization afforded by the multidentate ligands, when taken as a whole, the data presented here support a model in which the enhanced stabilization arises largely (if not solely) from the multidentate chelate effect.

Introduction

Surface-modified gold nanoparticles are used extensively as building blocks to construct mesoscopic structures for microelectronics,[1,2] catalysis,[3−6] receptor-based sensing (biological and chemical sensors),[7−15] SERS signal enhancement,[16−19] and ultrahigh-density data storage.[20,21] To maximize the efficiency of surface-modified gold nanoparticles in such applications, well-controlled particle size and efficient particle dispersion are necessary. The synthesis of gold nanoparticles via the citrate method[22] affords gold nanoparticles ranging from ∼2 to 100 nm, where the size can be tuned by adjusting the gold-to-citrate ratio.[23]

With the discovery and widespread use of self-assembled monolayers (SAMs) adsorbed onto metal colloids,[24,25] the surface composition of gold nanoparticles can now be modified to contain a variety of functional groups and even mixtures of functional groups.[24,26] By utilizing the highly specific interaction between alkanethiols and gold, researchers now have the ability to disperse small gold nanoparticles (i.e., <10 nm) into nonpolar solvents,[27−33] which allows for enhanced nanoparticle manipulation, including their deposition into ordered two-dimensional

(1) Sato, T.; Ahmed, H.; Brown, D.; Johnson, B. F. G. *J. Appl. Phys.* **1997**, *82*, 696−701.
(2) Klein, D. L.; McEuen, P. L.; Katari, J. E. B.; Roth, R.; Alivisatos, A. P. *Appl. Phys. Lett.* **1996**, *68*, 2574−2576.
(3) Haruta, M. *Catal. Today* **1997**, *36*, 153−166.
(4) Crooks, R. M.; Zhao, M.; Sun, L.; Chechik, V.; Yeung, L. K. *Acc. Chem. Res.* **2001**, *34*, 181−190.
(5) Andreeva, D.; Tabakova, T.; Idakiev, V.; Christov, P.; Giovanoli, R. *Appl. Catal. A* **1998**, *169*, 9−14.
(6) Valden, M.; Lai, X.; Goodman, D. W. *Science* **1998**, *281*, 1647−1650.
(7) Zhu, T.; Fu, X.; Mu, T.; Wang, J.; Liu, Z. *Langmuir* **1999**, *15*, 5197−5199.
(8) Pasquato, L.; Rancan, F.; Scrimin, P.; Mancin, F.; Frigeri, C. *Chem. Commun.* **2000**, 2253−2254.
(9) Reynolds, R. A., III.; Mirkin, C. A.; Letsinger, R. L. *J. Am. Chem. Soc.* **2000**, *122*, 3795−3796.
(10) Obare, S. O.; Hollowell, R. E.; Murphy, C. J. *Langmuir* **2002**, *18*, 10407−10410.
(11) Nath, N.; Chilkoti, A. *Anal. Chem.* **2002**, *74*, 504−509.
(12) Lin, S.-Y.; Liu, S.-W.; Lin, C.-M.; Chen, C.-h. *Anal. Chem.* **2002**, *74*, 330−335.
(13) Kim, Y.; Johnson, R. C.; Hupp, J. T. *Nano Lett.* **2001**, *1*, 165−167.
(14) Bartz, M.; Kuther, J.; Seshadri, R.; Tremel, W. *Angew. Chem., Int. Ed.* **1998**, *37*, 2466−2468.
(15) Naka, K.; Itoh, H.; Chujo, Y. *Langmuir* **2003**, *19*, 5496−5501.
(16) Orendorff, C. J.; Gole, A.; Sau, T. K.; Murphy, C. J. *Anal. Chem.* **2005**, *77*, 3261−3266.
(17) Xu, S.; Zhao, B.; Xu, W.; Fan, Y. *Colloid. Surf. A* **2005**, *257−258*, 313−317.
(18) Balmes, O.; Bovin, J.-O.; Malm, J.-O.; Xu, H. *Vib. Spectrosc.* **2005**, *37*, 189−193.
(19) Grabar, K. C.; Freeman, R. G.; Hommer, M. B.; Natan, M. J. *Anal. Chem.* **1995**, *67*, 735−743.
(20) Salazar-Alvarez, G.; Mikhailova, M.; Toprak, M.; Zhang, Y.; Muhammed, M. *Mater. Res. Soc. Symp. Proc.* **2002**, *704*, 169−175.
(21) Baur, C.; Bugacov, A.; Koel, B. E.; Madhukar, A.; Montoya, N.; Ramachandran, T. R.; Requicha, A. A. G.; Resch, R.; Will, P. *Nanotechnology* **1998**, *9*, 360−364.
(22) Frens, G. *Nature* **1973**, *241*, 20−22.
(23) *Colloidal Gold: Principles, Methods, and Applications*; Hayat, M. A., Ed.; Academic Press: San Diego, 1989; Vol. 1.
(24) Daniel, M.-C.; Astruc, D. *Chem. Rev.* **2004**, *104*, 293−346.
(25) Shon, Y.-S. In *Dekker encyclopedia of nanoscience and nanotechnology*; Schwarz, J. A., Ed.; Marcel Dekker: New York, 2004; pp 1−11.
(26) Ingram, R. S.; Hostetler, M. J.; Murray, R. W. *J. Am. Chem. Soc.* **1997**, *119*, 9175−9178.
(27) Brust, M.; Fink, J.; Bethell, D.; Schiffrin, D. J.; Kiely, C. *Chem. Commun.* **1995**, 1655−1656.
(28) Vijaya Sarathy, K.; Kulkarni, G. U.; Rao, C. N. R. *Chem. Commun.* **1997**, 537−538.
(29) Huang, S.; Sakaue, H.; Shingubara, S.; Takahagi, T. *Jpn. J. Appl. Phys. 1* **1998**, *37*, 7198−7201.
(30) Templeton, A. C.; Hostetler, M. J.; Kraft, C. T.; Murray, R. W. *J. Am. Chem. Soc.* **1998**, *120*, 1906−1911.

arrays.[29,34−37] In contrast, gold nanoparticles larger than ∼10 nm typically undergo irreversible flocculation during their modification with alkanethiols.[38,39] This type of aggregation proceeds via fusion of the metallic cores,[39] which are initially stabilized by electrostatic interactions. The aggregation, however, can be inhibited by slowing the removal of the charged species during displacement by the protecting thiol.[40−42] For example, the adsorption of Tween 20 or thioctic acid onto the nanoparticles prior to the adsorption of alkanethiols leads to a reduction in the extent of irreversible aggregation.[40,41] Separate studies have shown that gold nanoparticles can be stabilized by using thiols possessing negatively charged terminal groups (e.g., carboxylate-terminated alkanethiols),[43−45] but this type of electrostatic stabilization is limited to aqueous solutions.

It is likely that the enhanced aggregation observed for larger gold nanoparticles is due to their increased interparticle attraction, given that van der Waals forces are known to increase with particle size/mass.[33,39,46] To disperse large nanoparticles in nonpolar solvents, interparticle attraction can be overcome by generating short-range repulsion via increasing the conformational freedom of the surfactant layer.[47] Short-range repulsion between two particles can arise when the surfactant layers around the particles interpenetrate, giving rise to chain ordering and thus entropic loss.[33] For example, due to the repulsive, steric, and/or overlap forces between polymer-coated surfaces, many synthetic polymers and biopolymers (e.g., proteins, gelatin) have been used to prevent particle aggregation.[33,41] However, the polymer coatings are usually inhomogeneous, and the thickness is difficult to control.[47]

In efforts to overcome these difficulties, Wei and co-workers reported the stabilization of gold nanoparticles up to 87 nm using non-polymeric resorcinarene tetrathiols.[47] Compared to normal alkanethiols, these multidentate ligands offer enhanced nanoparticle stability in solution by effectively blocking aggregation of the particles through two possible mechanisms: (1) cooperative, multidentate binding of the surfactant onto the gold nanoparticles and (2) enhanced spacing between alkyl chains, corresponding to enhanced conformational freedom of the alkyl chains. Despite their promise, however, partial desorption and/or displacement via ligand exchange were observed during aging.[47] Furthermore, their molecular complexity and lengthy synthesis highlight the need for the development of simpler nonpolymeric stabilizing agents.

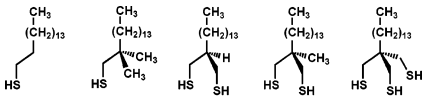

Figure 1. Structures of the adsorbates: normal hexadecanethiol (***n*-C16**), 2,2-dimethylhexadecane-1-thiol (**DMC16**), 2-tetradecylpropane-1,3-dithiol (**C16C2**), 2-methyl-2-tetradecylpropane-1,3-dithiol (**C16C3**), and 1,1,1-tris-(mercaptomethyl)pentadecane (***t*-C16**).

To this end, our group has been exploring the formation of conformationally disordered SAMs on gold via the adsorption of several new classes of multidentate alkanethiols (e.g., Figure 1).[48−51] In earlier studies on flat gold substrates, SAMs generated from 2-monoakylpropane-1,3-dithiols (**CnC2**),[49] 2-alkyl-2-methylpropane-1,3-dithiols (**CnC3**),[50] and 1,1,1-tris(mercaptomethyl)alkanes (***t*-Cn**)[51] showed lower chain packing densities compared to the densely packed SAMs generated from normal alkanethiols (**Cn**). Specifically, the molecular packing densities (and thus the conformational order of the alkyl chains) were observed to decrease according to the trend **Cn** ≫ **CnC2** > **CnC3** > ***t*-Cn**.[51] Furthermore, the stability of the SAMs against chemical desorption and displacement followed the exact opposite trend (i.e., the highly disordered films derived from ***t*-Cn** were the most robust).

For the purpose of the present study, we envisioned that the multidentate thiols would attach strongly to the surface of gold nanoparticles, with their loosely packed alkyl chains dangling in solution and stabilizing the nanoparticles entropically. Alternatively, we envisioned that the multidentate thiols might exert a stabilizing effect via their ability to bind to multiple sites on the surface of the gold nanoparticles (i.e., via the chelate effect, which is also entropic in nature).[52,53] Surprisingly, there has been no systematic study to distinguish the relative importance of these two effects in nanoparticle stabilization. Herein, we describe the dispersant properties of three thiol-based ligands having multidentate headgroups as shown in Figure 1: 2-tetradecylpropane-1,3-dithiol (**C16C2**), 2-methyl-2-tetradecylpropane-1,3-dithiol (**C16C3**), and 1,1,1-tris(mercaptomethyl)-pentadecane (***t*-C16**). We compare the stabilizing ability of these ligands to that of the monodentate ligands, hexadecanethiol (***n*-C16**), and 2,2-dimethylhexadecane-1-thiol (**DMC16**), where the latter ligand was designed to generate SAM-coated nanoparticles with reduced chain packing density similar to that of the multidentate thiols. Our studies find that only the multidentate ligands enable the extraction and dispersion of gold nanoparticles as large as 50 nm from the aqueous phase to a nonpolar organic phase; importantly, the multidentate-functionalized nanoparticles fail to undergo aggregation in the organic phase for at least 1 month at room temperature. Furthermore, a systematic analysis

(31) Porter, L. A., Jr.; Ji, D.; Westcott, S. L.; Graupe, M.; Czernuszewicz, R. S.; Halas, N. J.; Lee, T. R. *Langmuir* **1998**, *14*, 7378−7386.
(32) Isaacs, S. R.; Cutler, E. C.; Park, J.-S.; Lee, T. R.; Shon, Y.-S. *Langmuir* **2005**, *21*, 5689−5692.
(33) Israelachvili, J. *Intermolecular and Surface Forces*, 2nd ed.; Academic Press: New York, 1992.
(34) Mayya, K. S.; Caruso, F. *Langmuir* **2003**, *19*, 6987−6993.
(35) Chen, S. *Langmuir* **2001**, *17*, 2878−2884.
(36) Fernandez, C. A.; Wai, C. W. *J. Nanosci. Nanotechnol.* **2006**, *6*, 669−674.
(37) Lin, X. M.; Jaeger, H. M.; Sorensen, C. M.; Klabunde, K. J. *J. Phys. Chem. B* **2001**, *105*, 3353−3357.
(38) Weisbecker, C. S.; Merritt, M. V.; Whitesides, G. M. *Langmuir* **1996**, *12*, 3763−3772.
(39) Fujiwara, H.; Yanagida, S.; Kamat, P. V. *J. Phys. Chem. B* **1999**, *103*, 2589−2591.
(40) Lin, S.-Y.; Tsai, Y.-T.; Chen, C.-C.; Lin, C.-M.; Chen, C.-h. *J. Phys. Chem. B* **2004**, *108*, 2134−2139.
(41) Aslan, K.; Perez-Luna, V. H. *Langmuir* **2002**, *18*, 6059−6065.
(42) Bellino, M. G.; Calvo, E. J.; Gordillo, G. *Phys. Chem. Chem. Phys.* **2004**, *6*, 424−428.
(43) Yonezawa, T.; Kunitake, T. *Colloid. Surf. A* **1999**, *149*, 193−199.
(44) Yao, H.; Momozawa, O.; Hamatani, T.; Kimura, K. *Bull. Chem. Soc. Jpn.* **2000**, *73*, 2675−2678.
(45) Mayya, K. S.; Patil, V.; Sastry, M. *Langmuir* **1997**, *13*, 3944−3947.
(46) Evans, D. F. *The Colloidal Domain: Where Physics, Chemistry, Biology, and Technology Meet*, 2nd ed.; Wiley: New York, 1998.
(47) Balasubramanian, R.; Kim, B.; Tripp, S. L.; Wang, X.; Lieberman, M.; Wei, A. *Langmuir* **2002**, *18*, 3676−3681.
(48) Shon, Y.-S.; Lee, T. R. *J. Phys. Chem. B* **2000**, *104*, 8182−8191.
(49) Shon, Y.-S.; Colorado, R., Jr.; Williams, C. T.; Bain, C. D.; Lee, T. R. *Langmuir* **2000**, *16*, 541−548.
(50) Park, J.-S.; Smith, A. C.; Lee, T. R. *Langmuir* **2004**, *20*, 5829−5836.
(51) Park, J.-S.; Vo, A. N.; Barriet, D.; Shon, Y.-S.; Lee, T. R. *Langmuir* **2005**, *21*, 2902−2911.
(52) Li, X.-M.; de Jong, M. R.; Inoue, K.; Shinkai, S.; Huskens, J.; Reinhoudt, D. N. *J. Mater. Chem.* **2001**, *11*, 1919−1923.
(53) Pankau, W. M.; Monninghoff, S.; von Kiedrowski, G. *Angew. Chem., Int. Ed.* **2006**, *45*, 1889−1891.

of entropic stabilization vs chelate stabilization reveals that the latter effect is largely (if not solely) responsible for the observed enhancement in nanoparticle stabilization.

Experimental Section

Complete details regarding the materials, procedures, and instrumentation used to conduct the research reported here are provided as Supporting Information.

Results and Discussion

Brief Review of the Optical Properties of Metal Nanoparticles. According to Mie theory,[54] metallic nanoparticles with a radius much smaller than the incident wavelength of light will absorb strongly at certain wavelengths because of the resonant excitation of the surface plasmons. Furthermore, the position and intensity of the absorption bands are strongly influenced by particle size and shape, the surrounding medium, and the boundary conditions imposed by adjacent metallic particles. The surface plasmon resonance (SPR) band of gold spheres in aqueous solution appears at 525 nm. If, however, the colloidal particles aggregate, and the distance between aggregating particles becomes small compared with their radius, additional resonance bands will appear at longer wavelengths than those of the individual particles. Consequently, red-shifting and broadening of the resonances band are observed during aggregation.[38,39,41]

Kinetics of Aggregation of Thiol-Modified Gold Nanoparticles in Water/THF. During the process of SAM formation, hexadecanethiol (***n*-C16**) is known to displace citrate ions from the surface of gold nanoparticles, thereby reducing the surface charge.[55] Without strong charge−charge repulsion, gold nanoparticles modified with ***n*-C16** are driven to each other by van der Waals attraction,[33,46] leading to irreversible aggregation. As shown in Figure 2a, this type of aggregation gives rise to a dramatic red-shifting and broadening of the SPR band to 585 nm for gold nanoparticles having a diameter of 30 nm. Importantly, the rate of aggregation is much slower for gold nanoparticles modified by **DMC16**, **C16C2**, and **C16C3** when compared to ***n*-C16**. Specifically, Figure 2a shows that it takes only 1 h for the SPR band to shift to 550 nm after adding ***n*-C16**, and substantial aggregation occurs after 24 h, characterized by a severely broadened SPR band centered at 585 nm. In contrast, Figures 2b, 2c, and 2d show that the SPR band shifts to only 535 nm in 24 h after adding **DMC16**, **C16C2**, or **C16C3**. Moreover, Figure 2e shows a shift to only 532 nm in 24 h after adding tridentate ***t*-C16**; the latter shift occurs without any noticeable broadening of the SPR peak, suggesting that the gold nanoparticles undergo little or no aggregation upon adsorption of the tridentate alkanethiol.

We quantified the aggregation of thiol-functionalized gold nanoparticles using a semiempirical flocculation parameter,[38] defined as the integrated absorbance between 600 and 800 nm of the optical absorption spectra normalized to the absorption intensity of the surface plasmon peak. In this analysis, for example, increased absorption at 625 nm is associated with aggregation. As such, we monitored the extinction intensity at this wavelength to evaluate the aggregation process. As illustrated in Figure 3, the intensity of extinction at 625 nm

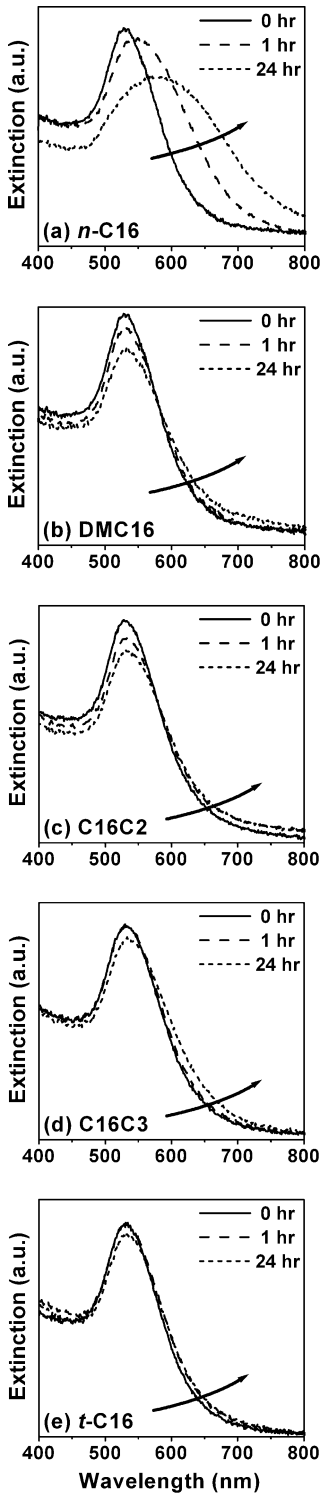

Figure 2. Time evolution of the UV−vis extinction spectra in 2:1 THF/water showing the stability of 30 nm gold nanoparticles modified with the indicated thiols: (a) ***n*-C16**, (b) **DMC16**, (c) **C16C2**, (d) **C16C3**, and (e) ***t*-C16**.

significantly increases for gold nanoparticles modified with ***n*-C16**, whereas a small change occurs for those modified with **DMC16**, **C16C2**, and **C16C3**. In contrast, for gold nanoparticles modified with ***t*-C16**, the intensity of this wavelength quickly reaches a plateau and remains constant. The small initial shift is probably due to the formation of the SAM on the surface of the gold nanoparticle.[11,56] The comparisons summarized here

(54) Mie, G. *Ann. Phys* **1908**, *25*, 377−445.
(55) Lin, M. Y.; Lindsay, H. M.; Weitz, D. A.; Ball, R. C.; Klein, R.; Meakin, P. *Phys. Rev. A* **1990**, *41*, 2005−2020.

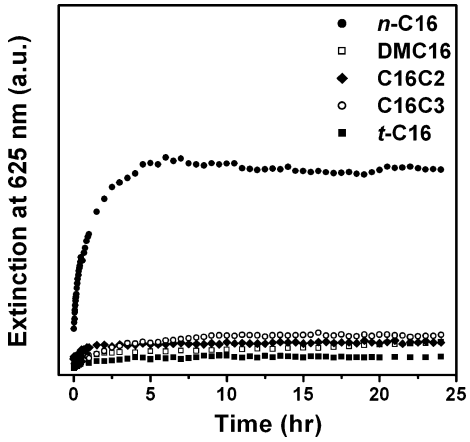

Figure 3. Time evolution of the extinction intensity at 625 nm in 2:1 THF/water of 30 nm gold nanoparticles modified with ***n*-C16**, **DMC16**, **C16C2**, **C16C3**, and ***t*-C16**.

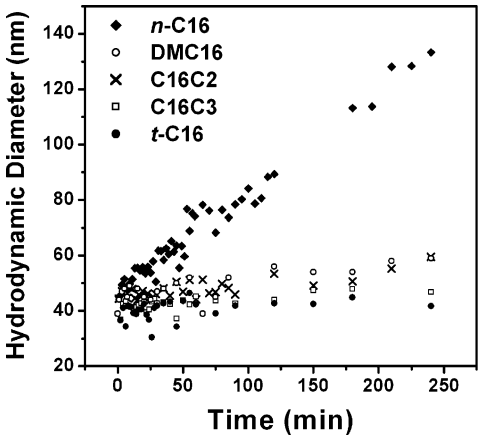

Figure 4. Kinetics of the aggregation of 30 nm gold nanoparticles modified with ***n*-C16**, **DMC16**, **C16C2**, **C16C3**, and ***t*-C16** as measured by dynamic light scattering (DLS) in 2:1 THF/water.

can be taken to indicate that ***t*-C16** is the most effective among the five adsorbates at stabilizing large gold nanoparticles in water/THF.

Analysis by DLS provides additional support for our interpretations of the UV−vis data. For example, Figure 4 shows that the addition of monodentate ***n*-C16** leads to a substantial increase in the hydrodynamic diameter, which is consistent with the proposed aggregation phenomenon. Furthermore, gold nanoparticles modified with the other adsorbates showed little or no increase in hydrodynamic diameter, indicating little or no aggregation (see Figure 4). Importantly, careful examination of the data in Figure 4 suggests that ***t*-C16** is the most effective ligand for preventing the aggregation of the nanoparticles in water/THF.

Another important observation from these studies centers on the stabilizing ability of **DMC16**: this ligand appears to be substantially better than ***n*-C16** and comparable to the multidentate thiols in stabilizing gold nanoparticles in water/THF. As noted above, gold nanoparticles generated by citrate reduction are stabilized by citrate-based charge−charge repulsion in aqueous solution.[23,57,58] Upon the addition of *n*-alkanethiol,

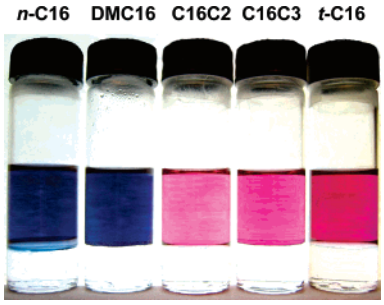

Figure 5. Photographs of 30 nm gold nanoparticles modified with ***n*-C16**, **DMC16**, **C16C2**, **C16C3**, and ***t*-C16** after phase transfer into 1:1 toluene/THF.

however, the citrate ions are typically displaced from the nanoparticle surface.[55] Although this process probably occurs to a substantial degree for **DMC16**, the displacement of citrate might be incomplete for this ligand. We note, for example, that compared with monodentate ***n*-C16** on gold, the monodentate **DMC16** ligand exhibits a markedly lower packing density (72% sulfur/chain density vs 100% for ***n*-C16**; see Supporting Information); furthermore, compared with the multidentate thiols **C16C2**, **C16C3**, and ***t*-C16**, the monodentate **DMC16** ligand is unable to chelate to the surface of gold. In XPS studies described below, we explore whether the stabilizing ability of **DMC16** in water/THF arises from the charge−charge repulsion of residual citrate ions trapped within void spaces on the surface of gold that are present only when using this adsorbate (vide infra).

Phase Transfer and Dispersion of Thiol-Modified Gold Nanoparticles in Organic Solution. Although many monodentate thiols are effective in dispersing and stabilizing small gold nanoparticles (~3 nm) in nonpolar solvents (e.g., hexanes, toluene, chloroform, or carbon tetrachloride),[59] these same thiols are typically ineffective in extracting and dispersing larger particles (>15 nm) in nonpolar solvents. Figure 5 provides additional evidence of this latter phenomenon, showing that ***n*-C16** and **DMC16** are poor dispersants and poor stabilizers of large gold nanoparticles (~30 nm in diameter). Although the ***n*-C16**- and **DMC16**-modified nanoparticles could be partially extracted into 1:1 toluene/THF with the help of TOAB, they aggregated rapidly, as indicated by the blue color of the solutions.[38,39,60] Interestingly, both ligands appear to be equally poor nanoparticle stabilizers in strictly organic solution; in water/THF, however, we observed that the aggregation of the **DMC16**-modified gold nanoparticles was much slower than that of ***n*-C16**-modified gold nanoparticles (vide supra).

In contrast to the monodentate thiols, the multidentate **C16C2**, **C16C3**, and ***t*-C16** are much more effective at extracting and dispersing the nanoparticles under the same conditions. Figure 5 shows that a few minutes after the addition of TOAB, the gold nanoparticles were transferred quantitatively to the organic phase, producing a solution having a pink or cherry-red color. Further analysis by UV−vis spectroscopy (Figure 6) shows that among all of the thiols examined, ***t*-C16** is the most effective dispersant, capable of extracting and stabilizing large gold nanoparticles in 1:1 toluene/THF in the presence of 5 mol % of TOAB per equivalent of thiol. Importantly, this latter dispersion was observed to be stable for at least 1 month at

(56) Aslan, K.; Luhrs, C. C.; Perez-Luna, V. H. *J. Phys. Chem. B* **2004**, *108*, 15631−15639.
(57) Enustun, B. V.; Turkevich, J. *J. Am. Chem. Soc.* **1963**, *85*, 3317−3328.
(58) Mirkin, C. A. *Inorg. Chem.* **2000**, *39*, 2258−2272.
(59) Park, J.-S. Ph.D. thesis, University of Houston, 2004.
(60) Link, S.; El-Sayed, M. A. *J. Phys. Chem. B* **1999**, *103*, 8410−8426.

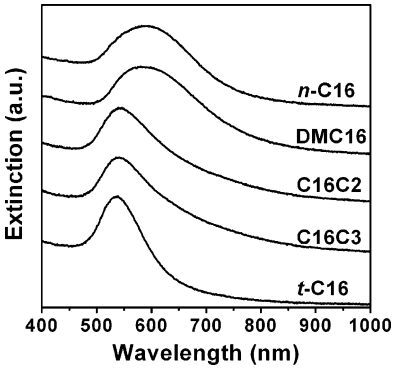

Figure 6. UV−visible extinction spectra of 30 nm gold nanoparticles modified with ***n*-C16**, **DMC16**, **C16C2**, **C16C3**, and ***t*-C16**, and phase-transferred into 1:1 toluene/THF.

room temperature with little or no change in the extinction band intensity or position.

Given the lower thiolate coverage on nanoparticles compared to that on flat gold substrates,[38] it is plausible that some citrate ions are retained around the gold nanoparticles after the addition of thiol, even when multidentate ligands are used. This phenomenon might rationalize why extractions without TOAB typically lead to only partial transfer of gold nanoparticles into the 1:1 toluene/THF phase.[61] The tetraalkylammonium cations can presumably neutralize residual citrate counterions,[62] enhancing the hydrophobic nature of the functionalized nanoparticle and facilitating the transfer from the aqueous phase to the organic phase. On the other hand, analysis by XPS of our SAM-coated nanoparticles reveals that citrate is present in measurable quantities only when **DMC16** is used as the stabilizing ligand (vide infra).

In the course of these studies, we observed also that the position of the SPR band of the gold nanoparticles (20−50 nm in diameter) was strongly influenced by the reaction conditions. The initial extinction band at 525 nm shifted slightly to 530 nm upon dispersion in 1:2 water/THF. Upon functionalization with ***t*-C16**, the SPR band shifted to 532 nm, and after phase transfer into 1:1 toluene/THF, it shifted further to 536 nm (see Figure 6). Theoretical predictions[63−65] and experimental observations[11,56] have also found that the position of the SPR band of colloidal gold is sensitive to the dielectric constant of the surrounding medium. Typically, the formation of a dielectric layer around a metallic nanoparticle or the incorporation into a medium with a higher refractive index shifts the SPR band to longer wavelength (lower energy).[11,56] Given that the refractive indices of water, THF, and toluene are 1.33, 1.41, and 1.50, respectively,[11] we can plausibly conclude that the observed shifts correspond to changes in the local environment of the gold nanoparticles, rather than to differences in flocculation. Furthermore, the absence of extinction intensity between 600 and 800 nm (see Figure 6) strongly suggests that the gold nanoparticles modified with the multidentate thiols (particularly ***t*-C16**) fail to aggregate to any substantial degree.

(61) We have also found that mixing TOAB in toluene with an aqueous solution of citrate gold in the absence of THF leads to flocculation of the nanoparticles rather than phase transfer.
(62) Survey scans by XPS of gold nanoparticles modified with multidentate thiols indicate the presence of nitrogen but not bromine.
(63) Kreibig, U.; Vollmer, M. *Optical properties of metal clusters*; Springer: New York, 1995.
(64) Mulvaney, P. *Langmuir* **1996**, *12*, 788−800.
(65) Eck, D.; Helm, C. A.; Wagner, N. J.; Vaynberg, K. A. *Langmuir* **2001**, *17*, 957−960.

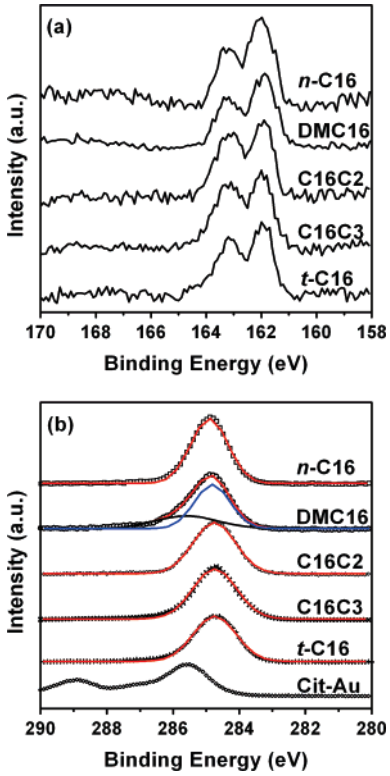

Figure 7. XPS spectra for 30 nm gold nanoparticles modified with ***n*-C16**, **DMC16**, **C16C2**, **C16C3**, and ***t*-C16** at: (a) S 2p region and (b) C 1s region (the solid lines are the results of curve fitting).

XPS Analysis of Thiol-Modified Gold Nanoparticles. XPS is highly useful in analyzing not only the nature of S−Au bonding, but also the atomic composition of SAMs on gold surfaces.[38,66,67] Although the sulfur signal can be significantly attenuated by the overlying alkyl chains (and thus lead to a low signal-to-noise ratio), analysis of the *S* 2p peak is a reliable method for evaluating the chemical bonding of sulfur atoms in SAMs.[38,66,67] In particular, it is known that photoelectron peaks with binding energies of 162.1 and 163.3 eV can be assigned to the *S* $2p_{3/2}$ and *S* $2p_{1/2}$ doublet, respectively, for sulfur atoms bonded to gold; in contrast, peaks at 164 eV can be assigned to unbound thiol species. The XPS data in Figure 7a show predominately the presence of bound sulfur with only a minimal signal (<15%) that can be attributed to unbound sulfur for the multidentate thiol-modified gold nanoparticles. This observation supports the notion of chelate stabilization[48−51] for these nanoparticles, which likely plays a role in their resistance to aggregation (vide infra).

Figure 7b shows the C 1s binding energies for the SAMs formed from each of the thiols. For each of the SAMs derived from ***n*-C16**, **C16C2**, **C16C3**, and ***t*-C16**, we observe a relatively narrow peak at ∼285 eV, which is characteristic of the alkyl groups of SAMs comprised largely of CH_2 units.[68] For the SAM derived from **DMC16**, however, the peak is broadened with an extended shoulder on the high-energy side, suggesting the presence of oxidized carbon species.[68] Numerical curve fitting indicates that there are at least two carbon species for this

(66) Lu, H. B.; Campbell, C. T.; Castner, D. G. *Langmuir* **2000**, *16*, 1711−1718.
(67) Laibinis, P. E.; Whitesides, G. M.; Allara, D. L.; Tao, Y. T.; Parikh, A. N.; Nuzzo, R. G. *J. Am. Chem. Soc.* **1991**, *113*, 7152−7167.
(68) Bain, C. D.; Troughton, E. B.; Tao, Y. T.; Evall, J.; Whitesides, G. M.; Nuzzo, R. G. *J. Am. Chem. Soc.* **1989**, *111*, 321−335.

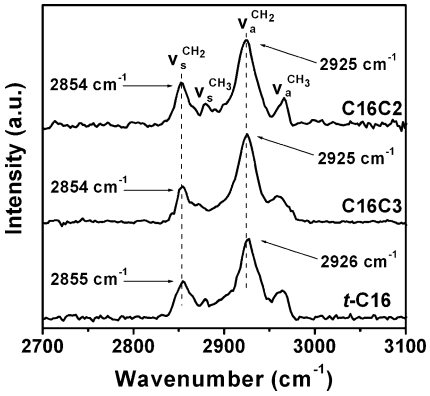

Figure 8. FT-IR spectra of 30 nm gold nanoparticles modified with **C16C2**, **C16C3**, and ***t*-C16** and dispersed in CCl_4.

adsorbate. Further comparison with the photoelectron spectrum of citrate-stabilized gold nanoparticles (Figure 7b, bottom) is consistent with a model in which there are citrate ions (or citrate derivatives) remaining on the surface of the gold nanoparticles after the adsorption of **DMC16**. As noted above, we propose that citrate ions fill void spaces on the surface of gold in the presence of **DMC16** and thereby lead to enhanced nanoparticle stabilization in water/THF. Further, it is plausible that citrate ions and void spaces exist only for the **DMC16** ligand due to its exclusive low surface density of both alkyl chains and sulfur atoms (i.e., 72 vs 100% for ***n*-C16**; see Supporting Information).

FTIR Analysis of Multidentate Thiol-Modified Gold Nanoparticles. We used transmission FTIR spectroscopy to evaluate whether the conformational order (or "crystallinity") of the pendant alkyl chains might play a role in the abilities of **C16C2**, **C16C3**, and ***t*-C16** to act as efficient dispersants and stabilizers. The C−H stretching region is known to be highly sensitive to the conformational order of the alkyl chains and the environment of the chains.[69] In particular, the degree of conformational order of alkyl chains can be estimated from the frequency and width of the methylene antisymmetric band ($\nu_a^{CH_2}$) and the methylene symmetric band ($\nu_s^{CH_2}$).[69−72] The methylene antisymmetric band ($\nu_a^{CH_2}$) of crystalline polyethylene appears at 2920 cm^{-1}, whereas that of liquid polyethylene appears at 2928 cm^{-1}; likewise, the methylene symmetric band ($\nu_s^{CH_2}$) of crystalline polyethylene appears at 2850 cm^{-1}, whereas that of liquid polyethylene appears at 2856 cm^{-1}.[69−72]

Figure 8 shows the transmission infrared spectra of gold nanoparticles modified with **C16C2, C16C3**, and ***t*-C16**. (*Note:* we were unable to obtain the corresponding infrared spectrum of gold nanoparticles modified with ***n*-C16** and **DMC16** because the gold nanoparticles aggregated irreversibly after mixing with these adsorbates and could not be dispersed into carbon tetrachloride). Gold nanoparticles modified with **C16C2** and dispersed in CCl_4 exhibited a $\nu_a^{CH_2}$ band at 2924.5 cm^{-1} and $\nu_s^{CH_2}$ band at 2853.5 cm^{-1}; those modified with **C16C3** showed a tiny but reproducible shift to lower frequency: $\nu_a^{CH_2}$ band at 2925.1 cm^{-1} and $\nu_s^{CH_2}$ band at 2853.7 cm^{-1}; and those modified with ***t*-C16** showed a small but reproducible shift to even lower frequency: $\nu_a^{CH_2}$ band at 2926.5 cm^{-1} and $\nu_s^{CH_2}$ band at 2855.4 cm^{-1}. These data suggest that the conformational order of the pendant alkyl chains decreases in the following order: **C16C2** > **C16C3** > ***t*-C16**. We note that the results obtained here are remarkably consistent with those found in previous reflectance IR studies of these SAMs on flat gold substrates.[51]

Origin of the Enhanced Stability Afforded by Multidentate Thiols. Given the stresses of flowing solution and/or interparticle collisions, stabilizing agents can move laterally on the surface of the nanoparticle while remaining attached, or they can simply desorb from the surface of the nanoparticle.[73] Stabilizers that are weakly anchored can, in fact, impart some stability to colloidal dispersions; such dispersions will flocculate as a result of stabilizer displacement or desorption. Some reports indicate that normal alkanethiolate-based SAMs desorb upon exposure to air[74−76] or upon heating to elevated temperatures (e.g., 70 °C) in a hydrocarbon medium.[54] Other reports show that adsorbed alkanethiolates can be readily displaced by approaching thiols.[68,77] Nevertheless, both the mobility and lability of surface-bound adsorbates depend strongly on the strength of binding of the adsorbate to the surface, which will vary with the number of adsorbate−surface bonds (i.e., monodentate vs bidentate vs tridentate).[51,78,79]

Alternatively, the concept of steric stabilization is widely used to rationalize the stabilization of colloidal particles by nonionic compounds. In these systems, steric repulsion arises largely from a loss of entropy in the surfactant layers due to the loss of chain mobility and increased torsional strain.[80] It is especially important in nonaqueous media, where electrostatic stabilization is less prevalent.[33,80] It can also be effective in media of high ionic strength because steric stabilizers are relatively insensitive to the presence of electrolytes.[33] Effective steric stabilizers combine both anchoring groups and stabilizing moieties. Anchoring groups perform most effectively if they are insoluble in the dispersion medium; in contrast, stabilizing moieties must be soluble in the dispersion medium to be effective.[80] Furthermore, theoretical modeling[33,72,81−83] and experimental observations[33,81] show that a high stabilizer density and a large adlayer thickness lead to enhanced steric stabilization.

To examine whether chelate stabilization or steric stabilization is the predominant factor in preventing the aggregation of thiol-modified nanoparticles, we first applied various known models of steric stabilization to our ligand system. Two stabilizing layers come into contact when particles approach one another at a separation distance less than twice the adlayer thickness (δ).

(69) Snyder, R. G.; Strauss, H. L.; Elliger, C. A. *J. Phys. Chem.* **1982**, *86*, 5145−5150.
(70) Bensebaa, F.; Ellis, T. H.; Badia, A.; Lennox, R. B. *J. Vac. Sci. Technol., A* **1995**, *13*, 1331−1336.
(71) Bensebaa, F.; Ellis, T. H.; Badia, A.; Lennox, R. B. *Langmuir* **1998**, *14*, 2361−2367.
(72) Porter, M. D.; Bright, T. B.; Allara, D. L.; Chidsey, C. E. D. *J. Am. Chem. Soc.* **1987**, *109*, 3559−3568.
(73) Napper, D. H. *J. Colloid Interface Sci.* **1977**, *58*, 390−406.
(74) Schoenfisch, M. H.; Pemberton, J. E. *J. Am. Chem. Soc.* **1998**, *120*, 4502−4513.
(75) Lee, M.-T.; Hsueh, C.-C.; Freund, M. S.; Ferguson, G. S. *Langmuir* **1998**, *14*, 6419−6423.
(76) Scott, J. R.; Baker, L. S.; Everett, W. R.; Wilkins, C. L.; Fritsch, I. *Anal. Chem.* **1997**, *69*, 2636−2639.
(77) Schlenoff, J. B.; Li, M.; Ly, H. *J. Am. Chem. Soc.* **1995**, *117*, 12528−12536.
(78) Shon, Y.-S.; Lee, T. R. *J. Phys. Chem. B* **2000**, *104*, 8192−8200.
(79) Garg, N.; Carrasquillo-Molina, E.; Lee, T. R. *Langmuir* **2002**, *18*, 2717−2726.
(80) Lewis, J. A. *J. Am. Ceram. Soc.* **2000**, *83*, 2341−2359.
(81) Vincent, B.; Edwards, J.; Emmett, S.; Jones, A. *Colloids Surf.* **1986**, *18*, 261−281.
(82) de Gennes, P. G. *Adv. Colloid Interface Sci.* **1987**, *27*, 189−209.
(83) Korgel, B. A.; Fullam, S.; Connolly, S.; Fitzmaurice, D. *J. Phys. Chem. B* **1998**, *102*, 8379−8388.

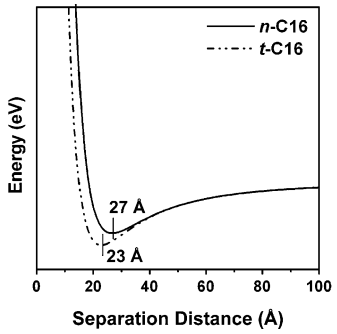

Figure 9. Calculated interparticle potential between two individual 30 nm gold nanoparticles modified with ***n*-C16** and ***t*-C16**.[83]

Bagchi[84,85] first proposed the stabilizer layers undergo compression rather than interpenetration, and Lambe et al.[86] further elaborated the denting mechanism. The corresponding elastic compression arises from a loss of configurational entropy of the stabilizer layer. To calculate the energy of the steric repulsion between alkanethiol-modified gold nanoparticles, we use the expression derived by de Gennes for two dense layers (brushes) of strongly adsorbed chains in a good solvent:[46,82,83]

$$E_{\text{steric}} \approx \frac{100R\delta^2}{(C-2R)\pi\sigma_{\text{thiol}}{}^3}\,kT\exp\left(\frac{-\pi(C-2R)}{\delta}\right) \quad (1)$$

where δ is the brush thickness (18 Å), σ_{thiol} is the diameter of the area occupied by the thiol on the particle surface, C is the center distance between nanoparticles, R is the particle radius, k is Planck's constant, and T is the temperature. Given that the surface area occupied by an *n*-alkanethiol molecule (e.g., ***n*-C16**) on gold is 21.4 Å^2, the corresponding distance between alkanethiolates on gold nanoparticles can be estimated to be 4.99 Å.[87] The surface area occupied by a trithiol (e.g., ***t*-C16**) is ~30 Å^2 based on measurements of surface coverage by XPS,[51] which leads to an average value of 5.88 Å for the distance between alkanetrithiolate chains on gold nanoparticles. Insertion of the respective values of σ_{thiol} into eq 1 shows that, in contrast to our observations, the higher packing density (i.e., smaller σ_{thiol}) of the ***n*-C16** SAMs should correlate with a stronger steric repulsion than that of the ***t*-C16** SAMs.

The interparticle interaction potential also includes the long-range London-van der Waals attraction. Using the expression derived by Hamaker:[88]

$$E_{\text{vdW}} = -\frac{A}{12}\left\{\frac{4R^2}{4R^2-C^2}+\frac{4R^2}{C^2}+2\ln\left[\frac{C^2-4R^2}{C^2}\right]\right\} \quad (2)$$

where A is the Hamaker constant (35×10^{-20} J for gold across hydrocarbon media).[33] Thus, the interaction potential ($E_{\text{steric}} + E_{\text{vdW}}$) between thiol-modified 300 Å gold nanoparticles can be calculated. Figure 9 shows that a weak attractive energy minimum exists at a separation distance of 27 and 23 Å for ***n*-C16** and ***t*-C16**, respectively, whereas the energy minimum of ***t*-C16** is steeper than that of ***n*-C16**. Clearly, this exercise demonstrates that the de Gennes model cannot rationalize why multidentate thiols afford enhanced stability against the aggregation of gold nanoparticles.

Given the liquid-like structure of adsorbed alkanethiol SAMs on nanoparticle surfaces,[31,59,83] an argument might arise that the disordered layers prefer interpenetration (the Vincent model)[81] rather than compression (the de Gennes model)[82] when nanoparticles approach one another. The steric interaction (E_{steric}) during their close approach is given by the interpenetration contribution ($E_{\text{steric,mix}}$) for $\delta < C < 2\delta$ and the interpenetration-plus-compression contribution ($E_{\text{steric,el}}$) for $C < \delta$.[73,81] We adopt the uniform segment model[81] to describe the interactions. In the domain $\delta < C < 2\delta$:

$$E_{\text{steric,mix}} = \frac{4\pi RkT}{\nu_1}\overline{\phi_2^{a2}}(0.5-\chi)\left(\delta-\frac{C}{2}\right)^2 \quad (3)$$

where ϕ_2^a is the average volume fraction of the segment in the adsorbed layer, χ (the Flory−Huggins parameter) is a measure of solvent quality, and ν_1 is the molar volume of the solvent. In the domain $C < \delta$, the value of E_{steric} is given by the summation of the mixing ($E_{\text{steric,mix}}$) and elastic ($E_{\text{steric,el}}$) terms:

$$E_{\text{steric,mix}} = \frac{4\pi R\delta^2 kT}{\nu_1}\overline{\phi_2^{a2}}(0.5-\chi)\left[\frac{C}{2\delta}-\frac{1}{4}-\ln\frac{C}{\delta}\right] \quad (4)$$

$$E_{\text{steric,el}} = \frac{2\pi R\delta^2 kT\rho_2\overline{\phi_2^a}}{M_2^a}\left\{\frac{C}{\delta}\ln\left[\frac{C}{\delta}\left(\frac{3-C/\delta}{2}\right)^2\right]-6\ln\left(\frac{3-C/\delta}{2}\right)+3\left(1-\frac{C}{\delta}\right)\right\} \quad (5)$$

where ρ_2 is the density and M_2^a is the molecular weight of the adsorbed species. Because SAMs on flat gold show decreased chain packing densities in the order: ***n*-C16** (normalized to 100%) ≫ **DMC16** (72%) > **C16C2** (64%) > **C16C3** (56%) > ***t*-C16** (51%),[51] it is reasonable to estimate that the average segment fractions on the nanoparticle surfaces follow the same order. Therefore, this model predicts the greatest steric repulsion for ***n*-C16** and the second greatest for **DMC16** under uniform conditions. We find, however, that ***n*-C16** and **DMC16** are the poorest stabilizers of gold nanoparticles in organic solution. As such, the Vincent model also fails to rationalize the superior ability of ***t*-C16** to prevent the aggregation of large gold nanoparticles.

Based on the Vincent model whereby stabilization arises due to the loss of entropy of the alkyl chains when nanoparticles approach one another, Wei and co-workers hypothesized that increasing the spacing between neighboring surfactant chains would significantly increase the conformational entropy of the surfactant layer and therefore increase interparticle repulsion entropically when the surfactant layers come into contact with one another.[47] The arguments presented in the preceding paragraph indicate, however, that this model is untenable for our chelating adsorbates and perhaps others.[47,52,89−92] Moreover, a broader examination of the FTIR data collected here further

(84) Bagchi, P. *J. Colloid Interface Sci.* **1974**, *47*, 86−99.
(85) Bagchi, P. *J. Colloid Interface Sci.* **1974**, *47*, 100−105.
(86) Lambe, R.; Tadros, T. F.; Vincent, B. *J. Colloid Interface Sci.* **1978**, *66*, 77−84.
(87) Sellers, H.; Ulman, A.; Shnidman, Y.; Eilers, J. E. *J. Am. Chem. Soc.* **1993**, *115*, 9389−9401.
(88) Hamaker, H. C. *Physica* **1937**, *4*, 1058−1072.
(89) Li, Z.; Jin, R.; Mirkin, C. A.; Letsinger, R. L. *Nucleic Acids Res.* **2002**, *30*, 1558−1562.
(90) Misra, T. K.; Chen, T.-S.; Liu, C.-Y. *J. Colloid Interface Sci.* **2006**, *297*, 584−588.
(91) Stavens, K. B.; Pusztay, S. V.; Zou, S.; Andres, R. P.; Wei, A. *Langmuir* **1999**, *15*, 8337−8339.
(92) Pankau, W. M.; von Kiedrowski, G.; Verbist, K. *Chem. Commum.* **2001**, 519−520.

disfavors the Vincent model. In particular, the observed trends in the shifts in the ν^{CH_2} band positions (observed here for gold nanoparticles and in ref 51 for flat gold) correlate with the observed trends in packing density determined by XPS on flat gold for these adsorbates (normalized to 100% for ***n*-C16**): **C16C2** (64%), **C16C3** (56%), and ***t*-C16** (51%).[51] The relative magnitude of the differences in conformational order/packing density suggests that we might expect to see differences in stability for gold nanoparticles coated with **C16C2** and **C16C3** (64% vs 56%), given that we readily see differences in stability for gold nanoparticles coated with **C16C3** and ***t*-C16** (56% vs 51%). The fact that we see no such difference for **C16C2** vs **C16C3** argues further against the Vincent model.

Upon consideration of all of the data and analyses discussed above, one physical phenomenon remains that can rationalize the enhanced stability afforded by the multidentate adsorbates—the well-known chelate effect.[93,94] This entropy-driven phenomenon rationalizes (i) the greater stabilizing ability of **C16C2** and **C16C3** vs ***n*-C16** and **DMC16** (bis-chelates vs mono-chelates), (ii) the similar stabilizing abilities of **C16C2** and **C16C3** (both bis-chelates), and (iii) the greater stabilizing ability of ***t*-C16** vs **C16C2** and **C16C3** (tris-chelate vs bis-chelates). We note that the desorption of multidentate SAMs requires the almost simultaneous breaking of all of the S−Au bonds, which is highly disfavored entropically. Moreover, given that alkanethiol-based SAMs on gold likely desorb from the surface as disulfides,[95] *intramolecular* desorption of the chelating adsorbates as cyclic disulfides will be energetically disfavored because of ring strain formed in the products.[96] Furthermore, *intermolecular* desorption as oligomeric disulfides is even more disfavored, requiring the concurrent desorption of four or more tethered sulfur atoms. Given that desorption of ligands from the surface of metal nanoparticles is directly attributable to nanoparticle aggregation,[97] we can reasonably conclude that the enhanced nanoparticle stabilization observed here when using the multidentate thiols is due to the chelate effect. Furthermore, we can reasonably argue that, in the absence of other extenuating factors, the chelate effect is the predominant stabilizing factor in other nanoparticle systems that utilize multidentate ligands.[47,52,89−92]

Conclusions

The work described here has demonstrated the successful dispersion and stabilization of large gold nanoparticles (20−50 nm) in solution through the use of multidentate thiol-based ligands, with the tridentate thiol ***t*-C16** being the most effective of the ligands examined. Analysis by XPS showed that most (>85%) of the sulfur moieties in the multidentate adsorbates are covalently bound to the surface of the gold nanoparticles. Although analysis by FTIR suggested that the conformational freedom of the alkyl chains might play an important role in preventing nanoparticle aggregation, other considerations argue strongly that the chelate effect is primarily responsible for the enhanced stabilization afforded by the multidentate adsorbates. Studies involving the use of these multidentate thiols to inhibit monolayer degradation in response to various applied stresses (e.g., electrochemical, photolytic, and corrosive or displacing agents) are currently underway.

Acknowledgment. We gratefully acknowledge financial support from the National Science Foundation (ECS-0404308 and DMR-0447588), the Texas Center for Superconductivity, and the Robert A. Welch Foundation (Grant E-1320). Use of the DLS device was made possible by a grant from the Department of Energy to Professor Simon Moss (UH). We also thank one reviewer for suggesting an insightful experiment.

Supporting Information Available: Experimental details regarding the materials, procedures, and instrumentation used to conduct the research reported here. These materials are available free of charge via the Internet at http://pubs.acs.org.

JA0724588

(93) Huheey, J. E. *Inorganic Chemistry*: *Principles of Structure and Reactivity*; Harper Collins: Singapore, 1983.
(94) Purcell, K. F.; Kotz, J. C. *Inorganic Chemistry*; W. B. Saunders: Philadelphia, 1977.
(95) Nuzzo, R. G.; Zegarski, B. R.; Dubois, L. H. *J. Am. Chem. Soc.* **1987**, *109*, 733−740.
(96) Burns, J. A.; Whitesides, G. M. *J. Am. Chem. Soc.* **1990**, *112*, 6296−6303.
(97) Corbierre, M. K.; Cameron, N. S.; Sutton, M.; Mochrie, S. G. J.; Lurio, L. B.; Ruhm, A.; Lennox, R. B. *J. Am. Ceram. Soc.* **2001**, *123*, 10411−10412.